Progress In Electromagnetics Research B, Vol. 94, 1–18, 2021

Negative Group Delay Prototype Filter Based on Cascaded Second Order Stages Implemented with Sallen-Key Topology

Miodrag Kandic* and Greg E. Bridges

Abstract—A Negative Group Delay (NGD) filter prototype design based on cascaded identical 2nd-order baseband stages is presented. The prototype design achieves an NGD-bandwidth product that in the upper asymptotic limit for a distributed design is a function of out-of-band gain in decibels raised to the power 3/4. This is an improvement of previous cascaded first-order designs that have an NGD-bandwidth functional dependency of out-of-band gain in decibels to the power of 1/2. The bandwidth is taken as the 3 dB amplitude response bandwidth. The corresponding NGD design upshifted to a non-zero center frequency, i.e., a Band-Stop Filter (BSF) design, is shown to be possible to implement with Sallen-Key topology, and an example is presented for a 500 MHz center frequency and a 100 MHz (20%) 3 dB bandwidth. The filter shows a 4.05 ns negative group delay with a 1.28 ns in-band variation and a 3-dB amplitude response over the bandwidth of 100 MHz, achieving an NGD-bandwidth product of 0.405. An in-band distortion metric is presented, which can be evaluated for any specified time-domain input waveform. It is shown that the bandwidth, order of filter and desired distortion for a particular input waveform are interrelated. Therefore, the proposed in-band distortion metric constitutes another trade-off quantity to be checked for any type of NGD design.

1. INTRODUCTION

Negative group delay (NGD) phenomenon is observed in media that support an abnormal wave propagation manifested by negative group velocity. In the frequency domain, NGD phenomenon is represented by a positive slope of the phase characteristic over a finite frequency band. In the time domain, when a pulse waveform is applied at the input of an NGD-exhibiting medium, the temporal location of the pulse peak at the output precedes the peak at the input. The necessary condition for pulse peak advancement at the output is that most of the frequency spectrum of the pulse waveform is contained within the NGD bandwidth of the medium, and that in-band amplitude and phase distortions do not significantly affect the pulse shape.

Propagation of electromagnetic waves through a medium with anomalous dispersion was initially studied by Sommerfeld and Brillouin [1], where a semi-infinite sinusoid input waveform with a defined "turn on" point in time, or "front", was considered. It was shown that the "front" velocity is always positive and exactly luminal under all circumstances, thus satisfying relativistic causality. Therefore, the group velocity does not correspond to the "front" velocity in such media, but merely characterizes the propagation of distinct features of a well-behaved wave packet, such as pulse maximum, as also discussed in [2]. The difference between the "front" velocity and group velocity was demonstrated in a medium with a slow group velocity [3]. In addition to NGD, other examples of abnormal wave propagation phenomena include superluminal [4], backward wave propagation (negative refractive index) [5], and simultaneous negative phase and group velocity [6]. Anomalous dispersion phenomena must exist within some frequency bands for all dispersive media, as a consequence of Kramers-Kronig relations which are applicable to all causal linear systems [7].

Received 12 July 2021, Accepted 5 September 2021, Scheduled 14 September 2021

* Corresponding author: Miodrag Kandic (Miodrag.Kandic@umanitoba.ca).
The authors are with Department of Electrical and Computer Engineering, University of Manitoba, 75A Chancellor's Circle, Winnipeg, Manitoba, R3T 5V6, Canada.

The work in Ref. [7] presents a proof showing that within a frequency band of abnormal propagation (such as NGD propagation), the magnitude of a causal medium response has a minimum, i.e., an out-of-band gain accompanies the in-band frequency region exhibiting abnormal propagation. If the in-band attenuation is gain-compensated by an amplifier for example, the out-of-band gain will cause undesired amplification of transients associated with propagation of pulses of finite duration, which have defined "turn on/off" points in time [8–10]. Such a distorted transient response will follow any points of discontinuity in the waveform or any of its derivatives, not just the "turn on/off" times [11]. The out-of-band gain is proportional to the medium's transient amplitude response and therefore it is an undesired trade-off quantity accompanying the NGD phenomenon [8, 9].

The trade-off relationship between the desired NGD-bandwidth product on one hand, and the undesired maximum out-of-band gain on the other hand, was quantified for selected type of media [8, 9]. For an infinitely distributed medium comprised of cascaded identical first-order circuits at baseband frequencies, or equivalently cascaded identical 2nd order single-tuned resonators at an up-shifted frequency band, the upper asymptotic limit of the NGD-bandwidth product was shown to be proportional to the square root of the out-of-band gain given in decibels [8]. Similarly, for an engineered causal medium with a flat in-band NGD characteristic, by obtaining the corresponding amplitude characteristic via Kramers-Kronig relations, the same square-root of the decibel out-of-band gain is derived for the upper asymptotic limit of the NGD-bandwidth product [9], just with a higher proportional factor compared to [8].

In this paper, as an extension of the work presented in [8] and [9], a medium characterized by cascaded identical second-order rational transfer functions at baseband frequencies is presented. The employed second-order transfer functions have complex zeroes and poles, and therefore cannot be expressed via cascaded first-order functions presented in [8] and [9]. It is shown that the frequency up-shifted equivalent of this design comprises of identical double-tuned resonators, i.e., 4th order rational transfer functions, and can be implemented via a Sallen-Key circuit topology. The upper asymptotic limit of the NGD-bandwidth product is shown to be proportional to the power of 3/4 of the out-of-band gain given in decibels, which is an improvement compared to the power of 1/2 relationship presented in [8] and [9]. Further, a combined amplitude-phase metric of in-band distortion, similar to the one presented in [12, 13], is discussed in this paper as another important NGD trade-off, in addition to the out-of-band gain. The useful NGD bandwidth is generally not as wide as the frequency band where the group delay characteristic is negative, or in high phase-distortion cases is not as wide as the band where the amplitude characteristic variation is within 3 dB. The discussed combined amplitude-phase distortion metric can be used to assess acceptable distortion level considering the input waveform applied, and the NGD bandwidth can be selected accordingly. Many reported NGD circuit designs [8, 14–26], can be assessed and compared, having the out-of-band gain and the in-band amplitude-phase distortion trade-offs in mind.

2. 2ND ORDER BASEBAND NGD DESIGN WITH COMPLEX ZEROS AND POLES

Designs reported in [8, 9] are based on identical cascaded 1st order rational transfer functions at baseband frequencies, which then when upshifted to a higher center frequency yield cascaded single-tuned identical 2nd order rational transfer functions. Alternatively, if a 2nd order baseband transfer function with complex zeros and poles ($\omega_{01} > \Delta\omega_1/2$, $\omega_{02} > \Delta\omega_2/2$) is considered, which therefore cannot be factorized as a product of 1st order functions with simple imaginary poles, the single stage transfer function becomes:

$$H(j\omega) = \frac{\omega^2 - j\Delta\omega_1\omega - \omega_{01}^2}{\omega^2 - j\Delta\omega_2\omega - \omega_{02}^2}. \tag{1}$$

The phase characteristic of the transfer function given in expression (1) is then evaluated as:

$$\varphi(\omega) = \tan^{-1}\left(\frac{-\Delta\omega_1\omega}{\omega^2 - \omega_{01}^2}\right) - \tan^{-1}\left(\frac{-\Delta\omega_2\omega}{\omega^2 - \omega_{02}^2}\right). \tag{2}$$

The group delay characteristic evaluated at the $\omega = 0$ center frequency is given by:

$$\tau(0) = -\left.\frac{d\varphi(\omega)}{d\omega}\right|_{\omega=0} = -\frac{\Delta\omega_1}{\omega_{01}^2} + \frac{\Delta\omega_2}{\omega_{02}^2}. \tag{3}$$

For this transfer function to exhibit an NGD at center frequency $\omega = 0$, one of the conditions that needs to be met is that the transfer function has a minimum (attenuation) at the center frequency, or in other words it exhibits an out-of-band gain of A ($A > 1$):

$$A = \omega_{02}^2/\omega_{01}^2, \tag{4}$$

which then yields $H(\infty) \to 1,\ H(0) = 1/A,\ A > 1$. Further, the expression for center frequency group delay obtained from expressions (3) and (4) yields:

$$\tau\left(0\right) = -\frac{\Delta\omega_1}{\omega_{01}^2} + \frac{\Delta\omega_2}{\omega_{02}^2} = -\frac{1}{\omega_{01}^2}\left(\Delta\omega_1 - \frac{\Delta\omega_2}{A}\right). \tag{5}$$

Since the center frequency group delay needs to be negative in NGD designs, from expression (5) it follows that the following condition needs to be met: $\Delta\omega_2 < A \cdot \Delta\omega_1$. Therefore, smaller $\Delta\omega_2$ yields larger NGD. Further, for the transfer function magnitude to be lower than $H(\infty)$ =1 over the entire frequency domain (ensuring maximum out-of-band gain stays at $1/H(0) = A$), it can be derived that the following condition needs to be met:

$$\Delta\omega_2 \geq \sqrt{2 \cdot \omega_{01}^2 \cdot (A-1) + \Delta\omega_1^2}. \tag{6}$$

Since smaller $\Delta\omega_2$ yields larger NGD as established by expression (5), in the interest of maximizing NGD the smallest value that satisfies inequality (6) is chosen, and the transfer function now becomes:

$$H\left(j\omega\right) = \frac{\omega^2 - j\omega \cdot \Delta\omega_1 - \omega_{01}^2}{\omega^2 - j\omega\sqrt{2 \cdot \omega_{01}^2 \cdot (A-1) + \Delta\omega_1^2} - A \cdot \omega_{01}^2}. \tag{7}$$

Further, for the transfer function to be monotonically increasing from the center frequency to higher frequency, it can be derived that $\Delta\omega_1 \geq \sqrt{2} \cdot \omega_{01}$ needs to be met. At the same time, to ensure complex zeros, $\Delta\omega_1 < 2 \cdot \omega_{01}$ is required as well, which together yields:

$$\sqrt{2} \cdot \omega_{01} \leq \Delta\omega_1 < 2 \cdot \omega_{01}. \tag{8}$$

Finally, for an optimized NGD-bandwidth product, the lower bound value of expression (8) is selected:

$$\Delta\omega_1 = \sqrt{2} \cdot \omega_{01}. \tag{9}$$

With the above:

$$H\left(j\omega\right) = \frac{\omega^2 - j\Delta\omega_1\omega - \omega_{01}^2}{\omega^2 - j\Delta\omega_2\omega - \omega_{02}^2} = \frac{\omega^2 - j\omega \cdot \sqrt{2} \cdot \omega_{01} - \omega_{01}^2}{\omega^2 - j\omega \cdot \sqrt{2A} \cdot \omega_{01} - A \cdot \omega_{01}^2}. \tag{10}$$

The transfer function now has only two parameters, out-of-band gain A and ω_{01} which is proportional to the 3-dB cut-off frequency. The 3-dB cut-off frequency derived from expression (10) yields (the condition $A > \sqrt{2}$ is needed for 3-dB bandwidth to exist):

$$\omega_c = \omega_{01} \cdot \frac{1}{\left(1 - \dfrac{2}{A^2}\right)^{1/4}}. \tag{11}$$

Example transfer function magnitude plots and associated group delay plots are shown in Fig. 1, for out-of-band gain values $A = 100$ (40 dB), 30 dB, 20 dB and 10 dB. The cut-off frequency of $\omega_c = 1$ is chosen, and parameter ω_{01} is back calculated from expression (11). For the 40 dB case, $\omega_{01} = \omega_c/1.0001 \approx 1$, $\Delta\omega_1 = \sqrt{2}$, $\omega_{02} = 10$, $\Delta\omega_2 = 10\sqrt{2}$. The plots in Fig. 1 demonstrate that requirements prescribed in the above derivation process are met for this 2nd-order transfer function with complex zeros and poles, such as monotonically increasing magnitude characteristic from its minimum at the center frequency, the 3-dB cut-off value at $\omega = 1$ as designed, NGD exhibited at the center frequency, etc. In the 40 dB example, a center frequency NGD of NGD $= -\tau(0) = 1.2729s$ is achieved, yielding an NGD-bandwidth product of NGD $\cdot\, \Delta f =$ NGD $\cdot\, \omega_c/\pi = 0.4052$.

It can be noted that as frequency increases from the center frequency, the group delay characteristic has a negative slope at first, before a slope reversal close to the 3-dB band edge.

As a contrast, 1st-order transfer functions (single stage, or cascaded) exhibiting NGD, such as those reported in [8, 9], have their group delay characteristic minimum at center frequency.

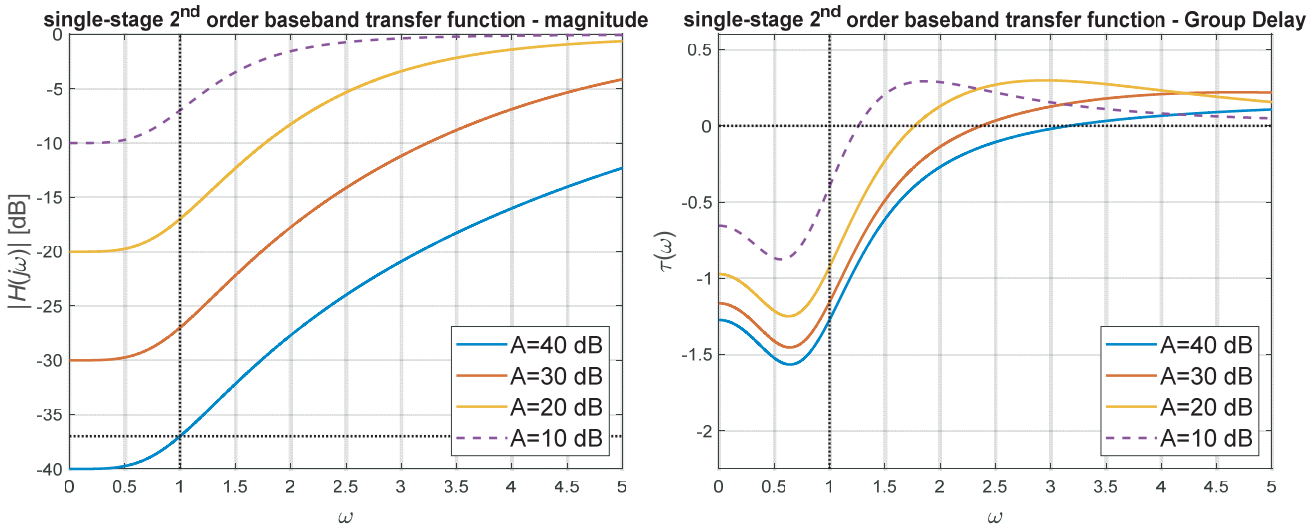

(a) (b)

Figure 1. Example 2nd-order baseband transfer function exhibiting NGD, (a) magnitude and (b) group delay plots.

3. BASEBAND NGD FILTER TRANSLATION TO BAND-STOP-FILTER (BSF)

To demonstrate a common variable substitution that transforms any baseband prototype transfer function to its translated equivalent at a higher, non-zero center frequency which still satisfies the condition $H(-j\omega) = H^*(j\omega)$, a 1st-order NGD baseband transfer function is considered first:

$$H_{BB1}(j\omega) = \frac{\omega - j\Delta\omega_1}{\omega - j\Delta\omega_2}. \tag{12}$$

To shift an NGD-exhibiting baseband transfer function to its BSF equivalent (with a finite band-stop attenuation), centered at a non-zero center frequency ω_0, the same frequency transformation that transforms a low-pass filter to its bandpass equivalent is applied (ω_c is the baseband 3-dB cut-off frequency, the bandwidth is $\Delta\omega = 2\omega_c$, and quality factor at ω_0 is $Q = \omega_0/\Delta\omega$):

$$\begin{aligned} \frac{\omega}{\omega_c} &\rightarrow Q \cdot \left(\frac{\omega}{\omega_0} - \frac{\omega_0}{\omega}\right) = \frac{\omega_0}{2\omega_c} \cdot \left(\frac{\omega}{\omega_0} - \frac{\omega_0}{\omega}\right) \\ \omega &\rightarrow \frac{1}{2}\left(\omega - \frac{\omega_0^2}{\omega}\right). \end{aligned} \tag{13}$$

Substituting expression (13) into the baseband transfer function $H_{BB1}(j\omega)$ expression (12), yields the corresponding BSF transfer function given by:

$$H_{BSF1}(j\omega) = \frac{\left(\omega - \omega_0^2/\omega\right)/2 - j\Delta\omega_1}{\left(\omega - \omega_0^2/\omega\right)/2 - j\Delta\omega_2} = \frac{\omega^2 - j2\Delta\omega_1\omega - \omega_0^2}{\omega^2 - j2\Delta\omega_2\omega - \omega_0^2}. \tag{14}$$

The transfer function above satisfies the criterion $H(-j\omega) = H^*(j\omega)$, and is the same form reported in [8, 9].

For the 2nd-order transfer function of interest in this paper, given by expression (1), application of the frequency transformation given by expression (13) yields the following baseband/BSF pair of transfer functions:

$$H_{BB2}(j\omega) = \frac{\omega^2 - j\Delta\omega_1\omega - \omega_{01}^2}{\omega^2 - j\Delta\omega_2\omega - \omega_{02}^2}. \tag{15a}$$

$$H_{BSF2}(j\omega) = \frac{\left(\omega^2 - \omega_0^2\right)^2 - j2\Delta\omega_1\omega\left(\omega^2 - \omega_0^2\right) - 4\omega_{01}^2\omega^2}{\left(\omega^2 - \omega_0^2\right)^2 - j2\Delta\omega_2\omega\left(\omega^2 - \omega_0^2\right) - 4\omega_{02}^2\omega^2}. \tag{15b}$$

The transfer function in expression (15b) satisfies the criterion $H(-j\omega) = H^*(j\omega)$. To determine poles and zeros of the shifted transfer function and factorize it, the following alternative form can be used:

$$H_{BSF2}(j\omega) = \frac{\omega^4 - j2\Delta\omega_1 \cdot \omega^3 - 2\left(\omega_0^2 + 2\omega_{01}^2\right) \cdot \omega^2 + j2\Delta\omega_1\omega_0^2 \cdot \omega + \omega_0^4}{\omega^4 - j2\Delta\omega_2 \cdot \omega^3 - 2\left(\omega_0^2 + 2\omega_{02}^2\right) \cdot \omega^2 + j2\Delta\omega_2\omega_0^2 \cdot \omega + \omega_0^4}. \tag{16a}$$

The factorized version of the 4th order function (16a) centered around frequency ω_0, which is more suitable for subsequent circuit design, is:

$$H_{BSF2}(j\omega) = \left(\frac{\omega^2 - j\Delta\omega_{1p}\omega - \omega_{01p}^2}{\omega^2 - j\Delta\omega_{2p}\omega - \omega_{02p}^2}\right) \cdot \left(\frac{\omega^2 - j\Delta\omega_{3p}\omega - \omega_{03p}^2}{\omega^2 - j\Delta\omega_{4p}\omega - \omega_{04p}^2}\right). \tag{16b}$$

where:

$$\omega_{01p}^2 = \omega_{01}^2 + K + \sqrt{2\omega_{01}^4 + \omega_0^2\left(2\omega_{01}^2 - \Delta\omega_1^2\right) + 2\omega_{01}^2 \cdot K} \tag{16c}$$

$$K = \sqrt{\omega_{01}^4 + \omega_0^4 + \omega_0^2\left(2\omega_{01}^2 - \Delta\omega_1^2\right)} \tag{16d}$$

$$\omega_{03p} = \frac{\omega_0^2}{\omega_{01p}}, \quad \Delta\omega_{1p} = \frac{2\Delta\omega_1\omega_{01p}^2}{\omega_0^2 + \omega_{01p}^2}, \quad \Delta\omega_{3p} = 2\Delta\omega_1 - \Delta\omega_{1p}. \tag{16e}$$

Similar expressions as (16c)–(16e) are used for computing denominator quantities in (16b), where index quantities in (16c)–(16e) containing '1' and '3' are replaced by '2' and '4', respectively.

As an example, consider the following 2nd order baseband transfer function exhibiting NGD (with out-of-band gain $A = 100$, and $\omega_c \approx \omega_{01} = 1$):

$$H_{BB3}(j\omega) = \frac{\omega^2 - j\sqrt{2}\omega - 1}{\omega^2 - j10\sqrt{2}\omega - 100}. \tag{17}$$

Employing (16c)–(16e) for the numerators and similar expressions for the denominators, the frequency up-shift to $\omega_0 = 10\omega_c = 10$ yields:

$$H_{BSF3}(j\omega) = \left(\frac{\omega^2 - j1.5142\omega - 10.734^2}{\omega^2 - j23.2439\omega - 21.4746^2}\right) \cdot \left(\frac{\omega^2 - j1.3142\omega - 9.3162^2}{\omega^2 - j5.0403\omega - 4.6567^2}\right). \tag{18}$$

The plot in Fig. 2 depicts the magnitude of the transfer function (18), with overall out-of-band gain $A = 40\,\text{dB}$ and bandwidth $\Delta\omega = 2\omega_c = 2$. A close in-band match is observed when compared with

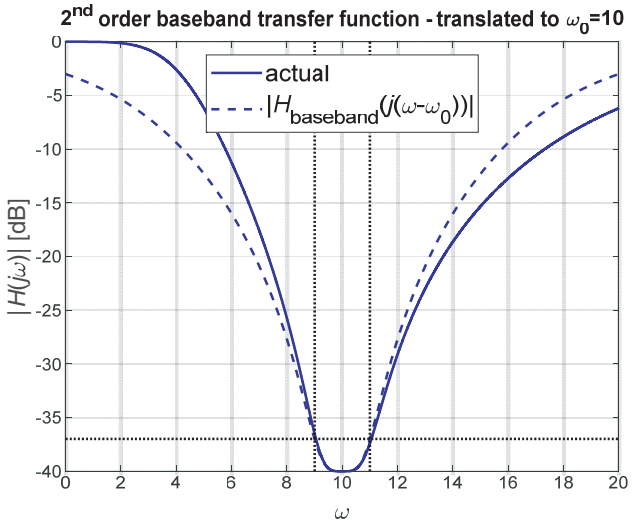

Figure 2. Example 2nd-order baseband transfer function magnitude response translated to $\omega_0 = 10\omega_c = 10$ center frequency and compared with a translated ideal baseband magnitude response.

the translated ideal baseband response. This transfer function achieves an NGD-bandwidth product of $\text{NGD} \cdot \Delta f = 0.4052$.

Note that the 2nd-order baseband transfer function with complex poles and zeros that is translated to its non-zero center frequency form (BSF with finite attenuation), cannot be realized exactly via cascaded/buffered passive resonators since the resonant frequencies (10.734 and 9.3162) in the numerators of the quadratic polynomials in expression (18) are not the same as the corresponding ones in the denominators (21.4746 and 4.6567). It is only the product of the resonant frequencies in the numerator, that is the same as the corresponding product in the denominator ($10.734 \times 9.3162 = 21.4746 \times 4.6567 = \omega_0^2 = 100$) as required in order to yield $H(0) = 1$. However, a particular version of the Sallen-Key topology presented next, has been found as able to achieve such a transfer function.

4. SALLEN-KEY TOPOLOGY

A generic Sallen-Key topology is depicted in Fig. 3, with four selectable impedances. For example, a well-known low-pass Sallen-Key design has capacitors in place of Z_F and Z_G impedances, and resistors in place of Z_1 and Z_2.

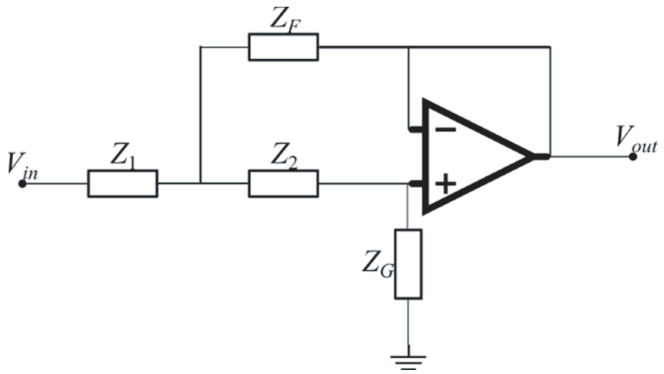

Figure 3. Generic Sallen-Key circuit topology.

The corresponding transfer function (V_{in} is assumed to be an ideal/buffered source), and input impedance are given by, respectively:

$$H(j\omega) = \frac{V_{out}}{V_{in}} = \frac{Z_G \cdot Z_F}{Z_G \cdot Z_F + Z_1 \cdot Z_2 + Z_F \cdot (Z_1 + Z_2)}, \tag{19}$$

$$Z_{in} = \frac{Z_G \cdot Z_F + Z_1 \cdot Z_2 + Z_F \cdot (Z_1 + Z_2)}{Z_F + Z_2}. \tag{20}$$

A Sallen-Key topology that can achieve the 2nd-order baseband transfer function with complex poles and zeros, translated to higher center frequency ω_0 as given by expression (16b), is shown in Fig. 4.

Consider an example design with out-of-band gain $A = 100 = 40\,\text{dB}$ and 3-dB bandwidth $\Delta\omega = 2\omega_c$. In the first step, parameters of the equivalent baseband design ($\Delta\omega_1$, $\Delta\omega_2$, ω_{01}, ω_{02}) are obtained from expression (10), as:

$$\begin{aligned} &\omega_{01} = \omega_c, \quad \Delta\omega_1 = \sqrt{2} \cdot \omega_c, \\ &\omega_{02} = \sqrt{A} \cdot \omega_c = 10 \cdot \omega_c, \quad \Delta\omega_2 = \sqrt{2A} \cdot \omega_c = 10\sqrt{2} \cdot \omega_c. \end{aligned} \tag{21a}$$

With the center frequency in this example related to 3-dB bandwidth as $\omega_0 = 10\omega_c = 5\Delta\omega$, or $Q = \omega_0/\Delta\omega = 5$, applying expressions (16c)–(16e) to obtain parameters of the transfer function expression (16b) centered around chosen ω_0, yields:

$$\begin{aligned} &\omega_{01p} = 1.0734\omega_0, \ \Delta\omega_{1p} = 0.15142\omega_0, \quad \omega_{03p} = 0.93162\omega_0, \ \Delta\omega_{3p} = 0.13142\omega_0, \\ &\omega_{02p} = 2.14746\omega_0, \ \Delta\omega_{2p} = 2.32439\omega_0, \quad \omega_{04p} = 0.46567\omega_0, \ \Delta\omega_{4p} = 0.50403\omega_0. \end{aligned} \tag{21b}$$

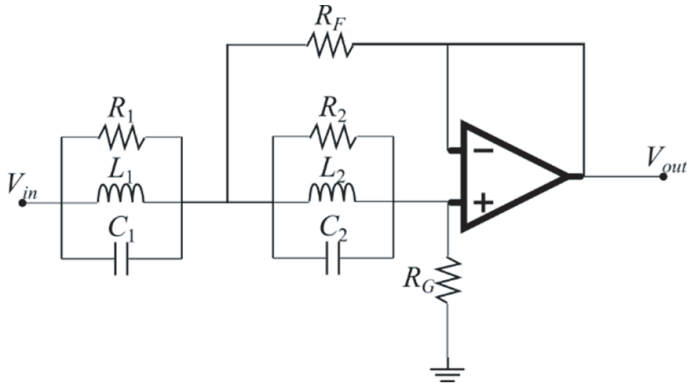

Figure 4. Sallen-Key topology that can be used to achieve the exact 2nd-order baseband NGD transfer function translated to a higher center frequency (BSF).

The component values of the design in Fig. 4 are obtained by equating the Sallen-Key transfer function (19), with the BSF transfer function (16b) and its parameters given by expression (21b). This will be demonstrated for a chosen center frequency design, chosen at $f_0 = 500\,\text{MHz}$, thus yielding a bandwidth of $\Delta f = f_0/5 = 100\,\text{MHz}$ (20%) in this example. First, a desired input impedance at center frequency is chosen, in this example $Z_{in} \approx 10Z_0 = 500\,\Omega$, such that loading effects are relatively small when a non-buffered source is used (or, if a shunt resistor is used to match the design closer to a non-buffered source impedance Z_0 within the bandwidth, having $Z_{in} \gg Z_0$ ensures the desired transfer function will not be affected considerably). Circuit component values are then calculated as:

$$R_1 \approx Z_{in} = 500\,\Omega, \tag{22a}$$

$$C_1 = \frac{1}{\Delta\omega_{1p}R_1} = 4.204\,\text{pF}, \quad L_1 = \frac{1}{\omega_{01p}^2 C_1} = 20.916\,\text{nH}, \tag{22b}$$

$$B = \frac{\Delta\omega_{2p} + \Delta\omega_{4p} - \Delta\omega_{1p} - \Delta\omega_{3p}}{(\Delta\omega_{2p} + \Delta\omega_{4p})\,\omega_0^2/\omega_{01p}^2 - \Delta\omega_{1p}\omega_{03p}^2/\omega_{01p}^2 - \Delta\omega_{3p}} = 1.1522,$$

$$C_2 = C_1\frac{B-1}{\left(1 - B\cdot\omega_{03p}^2/\omega_{01p}^2\right)} = 4.844\,\text{pF}, \quad L_2 = \frac{1}{\omega_{03p}^2 C_2} = 24.099\,\text{nH}, \tag{22c}$$

$$R_2 = \frac{1}{\Delta\omega_{3p}C_2} = 500\,\Omega, \quad R_G = \frac{1/C_1 + 1/C_2}{\Delta\omega_{2p} + \Delta\omega_{4p} - \Delta\omega_{1p} - \Delta\omega_{3p}} = 55.56\,\Omega, \tag{22d}$$

$$R_F = \frac{1}{\left(\omega_{02p}^2 + \omega_{04p}^2 + \Delta\omega_{2p}\Delta\omega_{4p} - \omega_{01p}^2 - \omega_{03p}^2 - \Delta\omega_{1p}\Delta\omega_{3p}\right) R_G C_1 C_2 - 1/R_1 - 1/R_2}$$

$$= 24.86\,\Omega. \tag{22e}$$

Using component values as calculated by expressions (22a)–(22e), as well as adding a shunt resistor at the input to approximately match the design to a $50\,\Omega$ source at the center frequency, yields the circuit topology depicted in Fig. 5.

The transmission coefficient ($S_{21} = V_{out}/V_S$) and group delay responses of the $50\,\Omega$-source driven Sallen-Key design shown in Fig. 5, along with the corresponding responses of the same design driven by an ideal, or buffered source, are shown in Fig. 6. Due to the relatively high values of the resonator resistors chosen ($10Z_0 = 500\,\Omega$), resistive match via a shunt resistor yields an in-band match close to the ideal source circuit, as expected. The center frequency NGD values are 4.05 ns and 3.85 ns, for the buffered and the resistor-matched designs, respectively. This 5% drop in NGD is attributed to a smaller out-of-band gain of the resistor-matched design due to its transfer function magnitude of roughly $-3\,\text{dB}$ at the out-of-band extremes as compared with $0\,\text{dB}$ of the buffered design.

As discussed, a Sallen-Key topology is required in order to achieve the exact up-shifted frequency design transfer function. However, alternative active or passive topologies involving two resonators

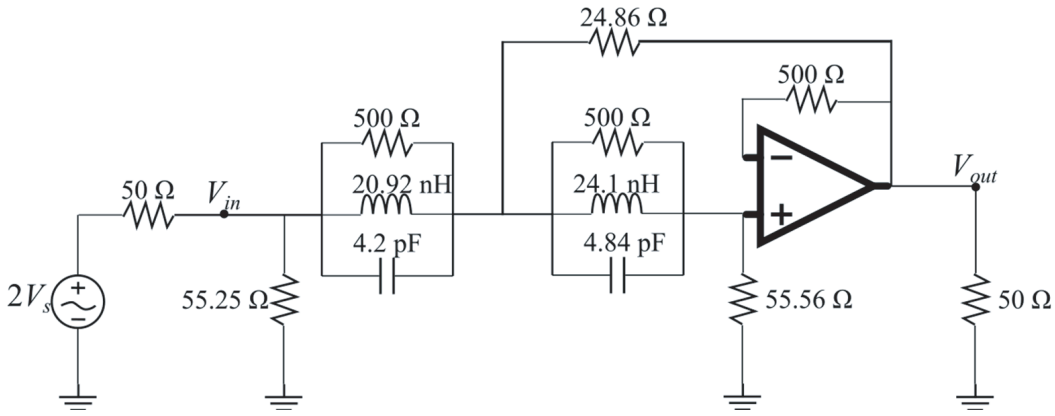

Figure 5. Sallen-Key topology design for the example transfer function given by expressions (16b) and (21b).

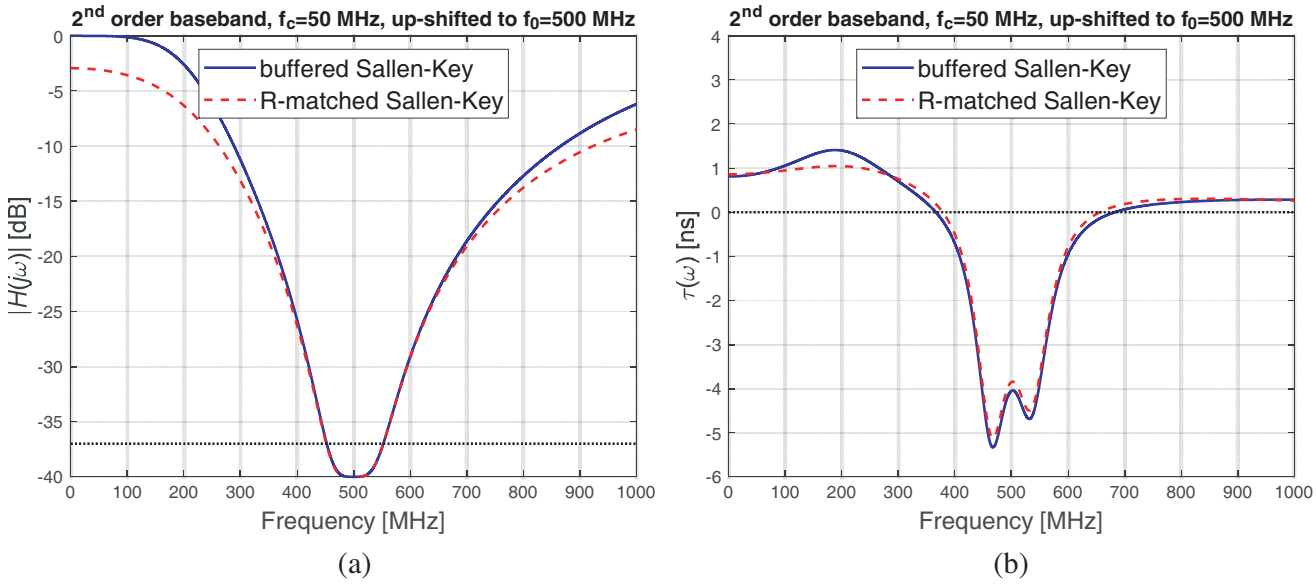

Figure 6. Transmission coefficient, (a) and group delay, (b) of the ideal source (buffered) driven Sallen-Key design, and of the shunt resistor matched design driven by a 50 Ω source.

(parallel and/or series) can still potentially achieve relatively good match to the exact transfer function. This can be achieved by keeping the two resonators' center frequencies and their individual bandwidths the same as in the Sallen-Key design (this keeps the numerator of the transfer function matched to the original design) while at the same time optimizing the resonators' individual resistor values to yield the smallest in-band transfer function deviation.

5. NGD-BANDWIDTH ASYMPTOTIC LIMIT OF CASCADED 2ND ORDER STAGES

Similar to the design with cascaded 1st order stages [8, 9], it is useful to express the NGD-bandwidth of the 2nd order cascaded design presented here as a function of the out-of-band gain trade-off quantity. As discussed in [8, 9], in addition to causing a center frequency attenuation for a passive design, the out-of-band gain in the frequency domain is directly proportional to the magnitude of undesired transients in the time domain, when waveforms/pulses with defined turn-on/off instances are used.

For a given overall out-of-band gain A, the transfer function of an N-stage cascaded (ideally

buffered) 2nd order baseband design is given by modifying single-stage design transfer function from expression (10), with each stage's individual out-of-band gain $A^{1/N}$, as:

$$H(j\omega) = \left(\frac{\omega^2 - j\omega \cdot \sqrt{2} \cdot \omega_{01} - \omega_{01}^2}{\omega^2 - j\omega \cdot \sqrt{2A^{1/N}} \cdot \omega_{01} - A^{1/N} \cdot \omega_{01}^2} \right)^N . \tag{23}$$

From expression (23), the baseband design 3-dB cut-off frequency can be derived as:

$$\omega_c = \omega_{01} \cdot \left(\frac{2^{1/N} - 1}{1 - \left(\frac{2}{A^2} \right)^{1/N}} \right)^{1/4} . \tag{24}$$

By choosing $\omega_c = 1$, expression (24) can be solved for parameter ω_{01} to be used in expression (23), for a given number of cascaded stages N. Such procedure yields transfer functions depicted in Fig. 7, for a fixed out-of-band gain $A = 100 = 40\,\text{dB}$, and number of stages $N = 1, 2, 3$.

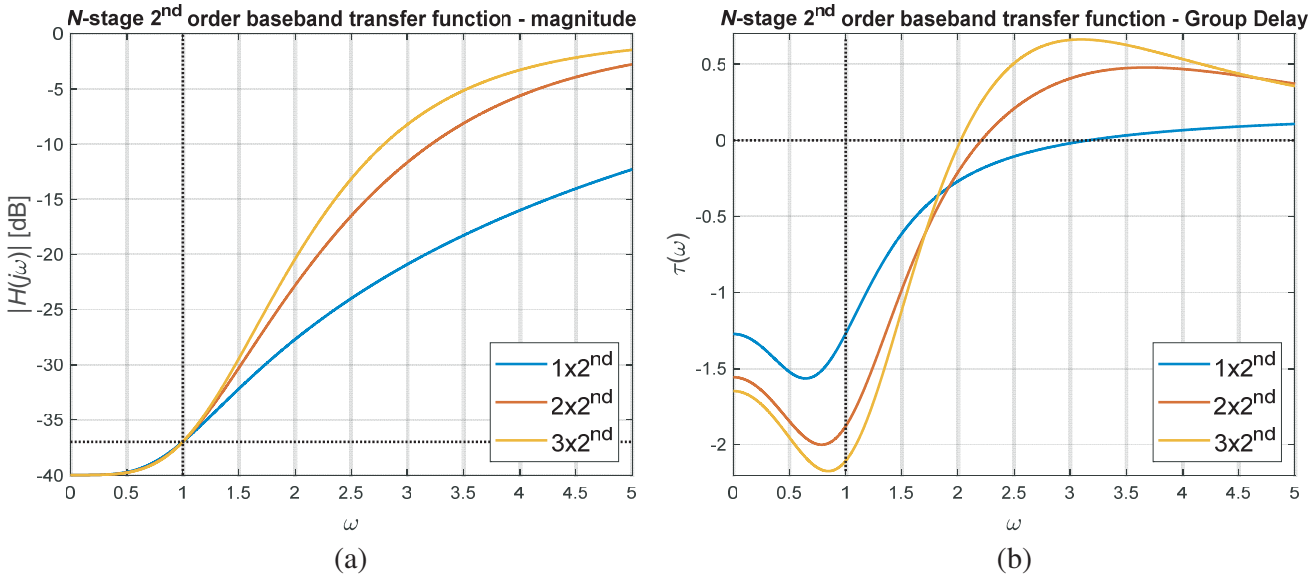

Figure 7. Examples of $N = 1$, 2 and 3-stage cascaded 2nd-order baseband transfer functions, (a) magnitude and (b) group delay.

From the N-stage baseband transfer function given by expression (23), the group delay at the center frequency is given by:

$$\begin{aligned} \tau(0) &= -N \frac{1}{\omega_{01}^2} \left(\Delta\omega_1 - \frac{\Delta\omega_2}{A^{1/N}} \right) = -N \frac{1}{\omega_{01}^2} \left(\sqrt{2}\omega_{01} - \frac{\sqrt{2A^{1/N}}\omega_{01}}{A^{1/N}} \right) \\ &= -N \frac{\sqrt{2}}{\omega_{01}} \left(1 - \frac{1}{A^{1/(2N)}} \right). \end{aligned} \tag{25}$$

The corresponding center frequency NGD-bandwidth product is then given by:

$$NGD \cdot \Delta f = NGD \cdot 2f_c \cdot \frac{\pi}{\pi} = -\tau(0) \cdot \frac{\omega_c}{\pi}. \tag{26}$$

Substituting expressions (24) and (25) into (26) yields a general expression for the NGD-bandwidth

product of N cascaded 2nd-order stages as:

$$(NGD \cdot \Delta f)_{N\_2nd} = N \cdot \frac{\sqrt{2}}{\pi}\left(1 - \frac{1}{A^{1/(2N)}}\right) \cdot \left(\frac{2^{1/N} - 1}{1 - \left(\frac{2}{A^2}\right)^{1/N}}\right)^{1/4}. \tag{27}$$

As a comparison, a topology consisting of $2N$ cascaded 1st order stages (yielding the same overall order as N cascaded 2nd order stages) exhibit NGD-bandwidth product given by [8]:

$$(NGD \cdot \Delta f)_{2N\_1st} = 2N \cdot \frac{1}{\pi}\left(1 - \frac{1}{A^{1/(2N)}}\right) \cdot \sqrt{\frac{2^{1/(2N)} - 1}{1 - \left(\frac{2}{A^2}\right)^{1/(2N)}}}. \tag{28}$$

Comparison of expressions (27) and (28) is depicted in Fig. 8, which shows that the cascaded 2nd-order design outperforms the cascaded 1st-order design (for the same overall order), in terms of higher NGD-bandwidth product for a given overall out-of-band gain.

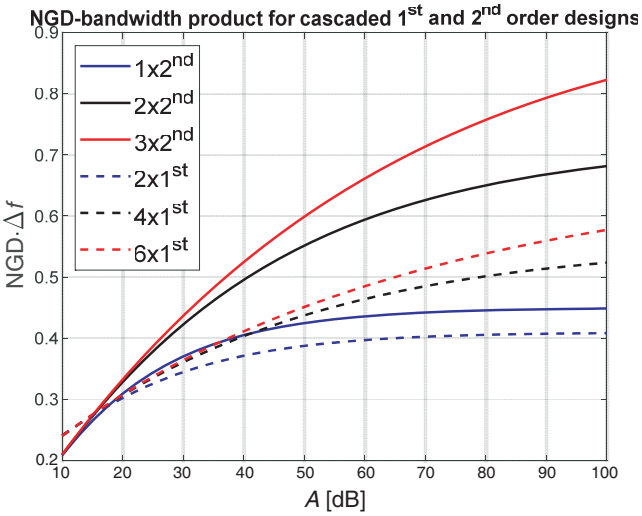

Figure 8. NGD-bandwidth product for cascaded 1st and 2nd order circuits, as a function of overall out-of-band gain.

Figure 9 depicts NGD-bandwidth product limit values as a function of overall out-of-band gain, for the two designs as the number of stages $N \to \infty$ (infinitely distributed case). For the infinitely distributed 1st order design ($N \to \infty$), the NGD-bandwidth product was derived to be [8]:

$$(NGD \cdot \Delta f)_{1st\_order} = \frac{\sqrt{\ln 2}}{\pi\sqrt{2}}\sqrt{\ln(A)} = \frac{1}{\pi}\sqrt{\frac{(\ln 2)\cdot(\ln 10)}{40}}\sqrt{A_{dB}}. \tag{29}$$

$$(NGD \cdot \Delta f)_{1st\_order} \approx 0.0636 \cdot \sqrt{A_{dB}}. \tag{30}$$

For the infinitely distributed 2nd order design ($N \to \infty$), the NGD-bandwidth product is derived from expression (27) to be:

$$(NGD \cdot \Delta f)_{2nd\_order} = \frac{1}{\pi}\frac{1}{\sqrt{2}}\left(\frac{\ln 2}{2}\right)^{1/4}\left(\frac{\ln 10}{20}\right)^{3/4} A_{dB}^{3/4}. \tag{31}$$

$$(NGD \cdot \Delta f)_{2nd\_order} \approx 0.0341 \cdot A_{dB}^{3/4}. \tag{32}$$

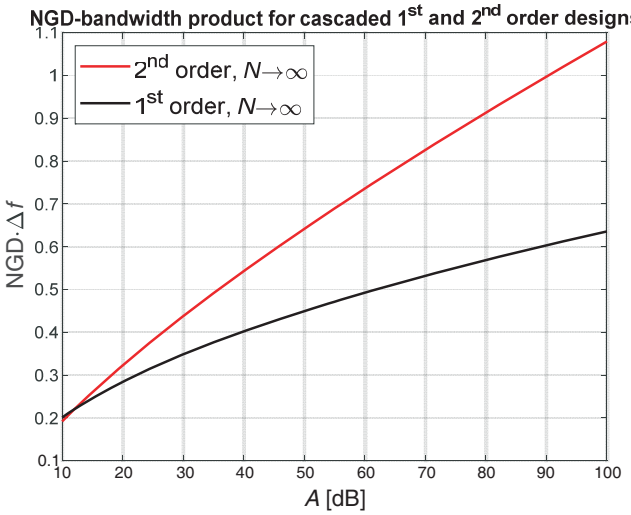

Figure 9. NGD-bandwidth product for infinitely distributed ($N \to \infty$) cascaded 1st and 2nd order circuits, as a function of overall out-of-band gain.

As an example, for a 40 dB out-of-band gain, an infinitely distributed 1st-order design yields an NGD-bandwidth product of 0.4021, while the 2nd-order design yields 0.5429 (about 35% larger). For an 80 dB out-of-band gain, the 1st-order design yields an NGD-bandwidth product of 0.5687, while the 2nd order design yields 0.9130 (about 60% larger).

In addition to the derived NGD-bandwidth asymptotic limit of an infinitely distributed medium comprised of cascaded 2nd-order stages as given by expressions (31) and (32), the baseband transfer function of the infinitely distributed medium can be derived from expression (23) as:

$$H_{BB}(j\omega) = \lim_{N\to\infty}\left(1+\frac{j\omega\cdot\sqrt{2}\cdot\omega_{01}\left(A^{1/(2N)}-1\right)+\omega_{01}^2\left(A^{1/N}-1\right)}{\omega^2-j\omega\cdot\sqrt{2A^{1/N}}\cdot\omega_{01}-A^{1/N}\cdot\omega_{01}^2}\right)^N$$
$$= \exp\left(\ln(A)\,\frac{j\omega\cdot\omega_{01}/\sqrt{2}+\omega_{01}^2}{\omega^2-j\omega\cdot\omega_{01}\cdot\sqrt{2}-\omega_{01}^2}\right). \tag{33a}$$

The relationship of the parameter ω_{01} in Equation (33a) to the 3-dB cut-off frequency of the distributed medium can be derived from expression (24) as:

$$\omega_{01} = \omega_c\cdot\left(\frac{1-\left(\frac{2}{A^2}\right)^{1/N}}{2^{1/N}-1}\right)^{1/4} = \omega_c\cdot\left(\frac{2\ln(A)}{\ln 2}-1\right). \tag{33b}$$

The infinitely distributed medium transfer function expression (33a) is corroborated in Fig. 10, which shows a fast convergence to the distributed medium for the number of stages as low as $N = 5$. For the distributed medium up-shifted version to a higher center frequency ω_0, the same substitution given by expression (13) can be applied to (33a), yielding:

$$H_{BSF}(j\omega) = \exp\left(\ln(A)\,\frac{j\sqrt{2}\omega\cdot\left(\omega^2-\omega_0^2\right)\cdot\omega_{01}+4\omega_{01}^2\cdot\omega^2}{\left(\omega^2-\omega_0^2\right)^2-j2\sqrt{2}\omega\cdot\left(\omega^2-\omega_0^2\right)\cdot\omega_{01}-4\omega_{01}^2\cdot\omega^2}\right). \tag{34}$$

There is a proportional relationship between the out-of-band gain and the magnitude of transients, when pulses with finite turn-on/off times propagate in an NGD medium [8, 9]. Therefore, for two media exhibiting the same out-of-band gain, the same magnitude of transients is expected. This is shown in Fig. 11 for the 1st-order and 2nd-order infinitely distributed baseband NGD designs. Both example

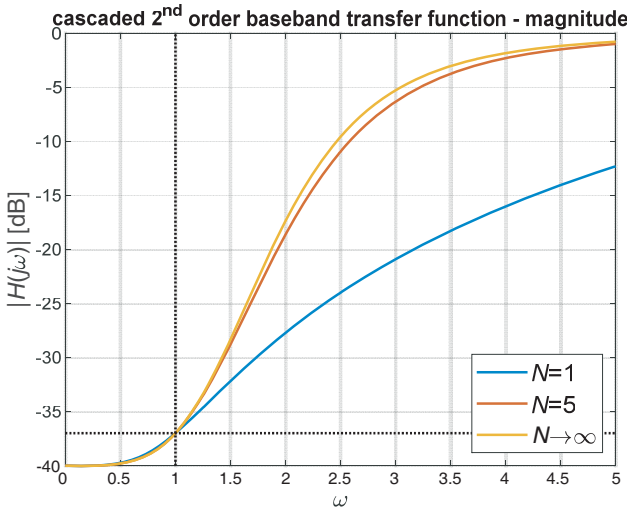

Figure 10. Transfer function of different number of cascaded 2nd order stages and its convergence to an infinitely distributed medium.

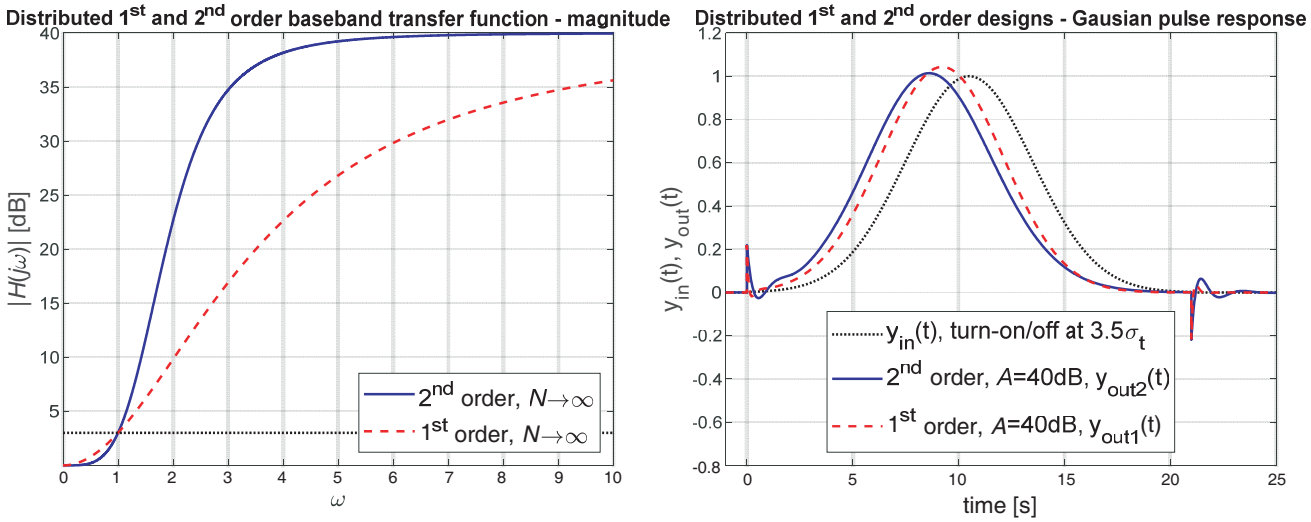

(a) (b)

Figure 11. Infinitely distributed 1st-order and 2nd-order baseband transfer function, (a) magnitude responses, and (b) time-domain responses to a Gaussian pulse turned-on/off at $3.5\sigma_t$.

designs are chosen to have an out-of-band gain of 40 dB ($A = 100$), with center frequency magnitude response fully gain-compensated (0 dB). This example is chosen so that the time-domain response pulse peaks are close in magnitude to the input pulse peak. The input pulse to both designs shown in Fig. 11 is a Gaussian pulse with its frequency spectrum standard deviation corresponding to 1/3 of the 3-dB bandwidth cut-off frequency ($\sigma_\omega = \omega_c/3$), and the turn-on/off times chosen at $3.5\sigma_t$ ($\sigma_t = 1/\sigma_\omega$). The input pulse value at the selected turn-on/off times is $\exp(-3.5^2/2) \approx 0.0022$ of the peak value, and subsequently the transient magnitude is expected to be amplified by $A = 100$, to 0.22 of the peak value, as corroborated in Fig. 11. Therefore, for the same out-of-band-gain, and thus the same transient's magnitude, a 2nd-order NGD medium can achieve larger pulse peak advancement compared to the corresponding 1st-order medium. The transient settling time, however, is longer for the 2nd-order medium, as observed after the turn-off time in Fig. 11(b).

6. NGD-BANDWIDTH PRODUCT AND OUT-OF-BAND GAIN FIGURE OF MERIT

The trade-off between the NGD-bandwidth product and the undesired out-of-band gain can be captured by a Figure of Merit (FOM), defined here as the ratio of the two trade-off quantities:

$$FOM = \frac{NGD \cdot BW}{A_{dB}}. \tag{35}$$

For example, FOM values for the infinitely distributed 1st and 2nd-order circuits discussed in the previous section are functions of out-of-band gain, as given by:

$$FOM_{2nd\_order\_distr} = \frac{0.0341}{A_{dB}^{1/4}}, \quad FOM_{1st\_order\_distr} = \frac{0.0636}{A_{dB}^{1/2}}. \tag{36}$$

For an out-of-band gain of 20 dB for example, FOM values of the 2nd and 1st-order infinitely distributed circuits are 0.0161 and 0.0142, respectively, with an approximate 13% FOM difference in favor of the 2nd order circuit. For a 40 dB out-of-band gain, the FOM difference increases to 35%. Since the FOM varies with out-of-band gain, to meaningfully compare the performance of different types of NGD circuits, their respective FOM values should be compared for same out-of-band gain. Further, the NGD bandwidth (BW) used in the FOM calculation (35) should be either the 3-dB amplitude characteristic bandwidth, or even a smaller bandwidth in the case of a high combined amplitude-phase in-band distortion, as discussed in the next section. Note that using the entire bandwidth over which the group delay is negative, as done in some publications, would generally yield an unacceptable level of distortion. For example, as per Fig. 7(b), considering such bandwidth would result in approximately 20 dB in-band amplitude variation.

7. IN-BAND DISTORTION METRIC

In addition to frequency-domain out-of-band gain which is proportional to the magnitude of time-domain transients [8, 9], another NGD trade-off quantity is distortion of the steady-state portion of a time-domain input waveform. This distortion is due to in-band phase non-linearity (non-constant group delay), as well as non-constant magnitude response within the 3 dB bandwidth.

For a general input time-domain waveform $f(t)$, with its frequency spectrum given by $F(j\omega)$, an in-band combined amplitude/phase distortion metric for a baseband transfer function $H(j\omega)$ can be evaluated in a similar manner as that proposed in [12, 13]:

$$D_{\text{in-band}} = \sqrt{\frac{\int_0^{\omega_c} \left| F(j\omega) - e^{-j\omega\Delta t_{pk}} \cdot F(j\omega) \cdot H(j\omega) \cdot |f(t)|_{\max} / |y(t)|_{\max} \right|^2 d\omega}{\int_0^{\omega_c} |F(j\omega)|^2 \, d\omega}}. \tag{37}$$

Here Δt_{pk} is the resulting time-domain advancement of the waveform peak, ω_c is the 3 dB cut-off, while $|f(t)|_{\max}$ and $|y(t)|_{max}$ are the respective magnitudes of the input and output peaks. Since linear scaling and time shift of a waveform does not contribute to distortion, the output spectrum in the numerator of expression (37), $F(j\omega) \cdot H(j\omega)$, is scaled and shifted to match the magnitude and position of the input waveform peak. In the distortion metric proposed in expression (37), the output spectrum scaling and shifting used is based on the exact observed time-domain output pulse peak magnitude and time-shift. Conversely, in [12, 13] the output spectrum scaling and shifting are approximated by the center frequency magnitude and group delay response values, i.e., $|f(t)|_{\max}/|y(t)|_{\max} \approx 1/H(0)$ and $\Delta t_{pk} \approx -\tau(0)$, respectively. The distortion metric in expression (37) is more easily evaluated in the frequency domain since it involves finite integral bounds over half of the bandwidth (due to symmetry). An equivalent evaluation in the time domain would involve infinite bounds, since chopping the frequency spectrum at a finite frequency ω_c results in a waveform over the entire time-domain.

As an example, the distortion metric is examined for a Gaussian pulse input waveform with a frequency spectrum standard deviation equal to 1/6th of the NGD 3 dB-bandwidth (its time-domain

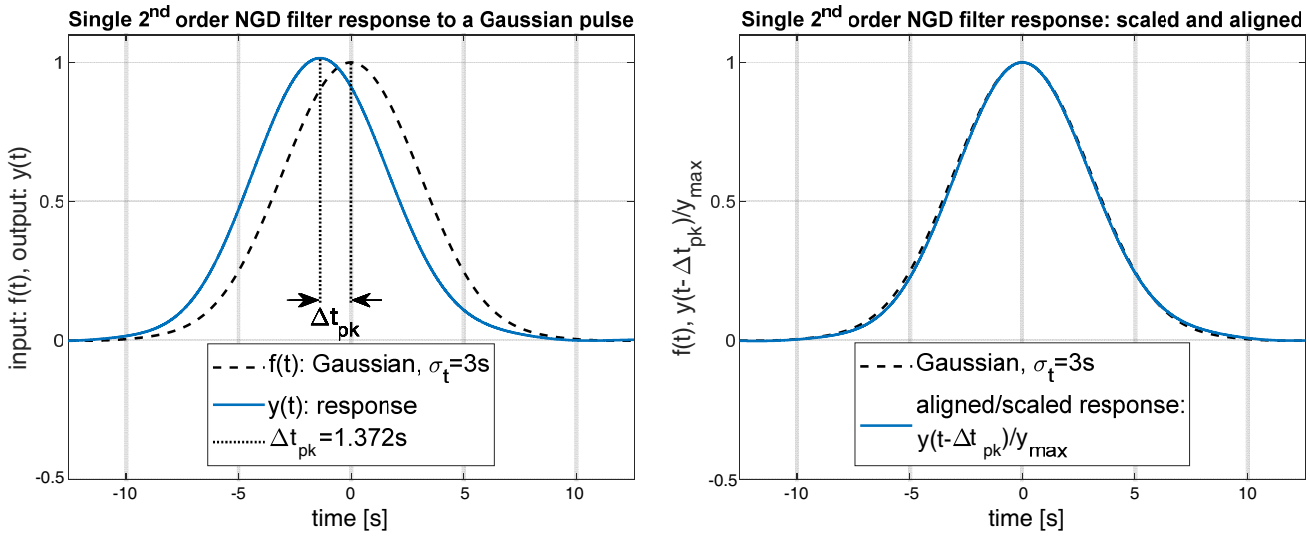

Figure 12. (a) Input Gaussian pulse with a frequency spectrum cut-off at $\omega_c = 1$, and the corresponding output waveform of a single 2nd-order stage gain-compensated design. (b) The same comparison but with the output waveform shifted by Δt_{pk} and normalized by $|y(t)|_{\max}$.

standard deviation is given by $\sigma_t = 1/\sigma_\omega = 6/\Delta\omega = 3/\omega_c = 3/(\pi\Delta f))$. If this waveform is applied as an input to a single stage 2nd-order NGD baseband transfer function, from expression (37) the distortion metric is $D_{\text{in-band-Gaussian}} = 0.0217$. As a comparison, for the 1st-order low-pass filter design $D_{\text{low-pass-Gaussian}} = 0.0411$, which is about 89% larger. Fig. 12 illustrates the input and output waveforms for the single stage 2nd-order example, with a chosen $\omega_c = 1$ and $A = 40\,\text{dB}$. This is a gain-compensated ($H(0) = 1$) version of the design with magnitude and group delay characteristics previously shown in Fig. 1.

The center frequency NGD of $-\tau(0) = 1.2729\,\text{s}$ (NGD-bandwidth product of 0.4052) is close but not exactly equal to the time-domain advancement of the Gaussian pulse shown in Fig. 12, where $\Delta t_{pk} = 1.372$.

The next case considered is a sinc function input, $f(t) = \sin(\omega_c t)/(\omega_c t)$, with its peak magnitude $|f(t)|_{\max} = f(t \to 0) = 1$. This case is expected to represent a worse case scenario, as it equally encompasses magnitude and phase distortion over the entire 3 dB-bandwidth. The corresponding frequency spectrum is constant within the bandwidth, $F(j\omega) = \pi/\omega_c$. The distortion metric, expression (37), can be simplified as:

$$D_{\text{in-band-sinc}} = \sqrt{\frac{1}{\omega_c}\int_0^{\omega_c} \left|1 - e^{-j\omega\Delta t_{pk}} \cdot H\left(j\omega\right)/\left|y(t)\right|_{\max}\right|^2 d\omega}. \tag{38}$$

When the sinc function is applied as input to a single stage 2nd-order NGD baseband transfer function, the distortion is $D_{\text{in-band-sinc}} = 0.1072$. As a comparison, for the 1st-order low-pass filter design the corresponding $D_{\text{low-pass-sinc}} = 0.1093$, which is about 2% higher. Fig. 13 illustrates the input and output waveforms for the single stage 2nd-order NGD gain-compensated design, with a chosen $\omega_c = 1$ and out-of-band gain $A = 40\,\text{dB}$.

In both examples in Figs. 12 and 13, the distortion metric for the waveforms applied to a single stage 2nd-order circuit is less than it would be for a 1st-order low-pass filter. However, this may not be the case for certain multi-stage cascaded designs or for certain out-of-band gains, since the distortion increases with the number of stages N, as well as with the out-of-band gain A. To examine this, we consider the infinitely distributed cascaded 2nd order design ($N \to \infty$). Fig. 14 gives the NGD-bandwidth product as a function of the out-of-band decibel gain. In addition to the NGD evaluated

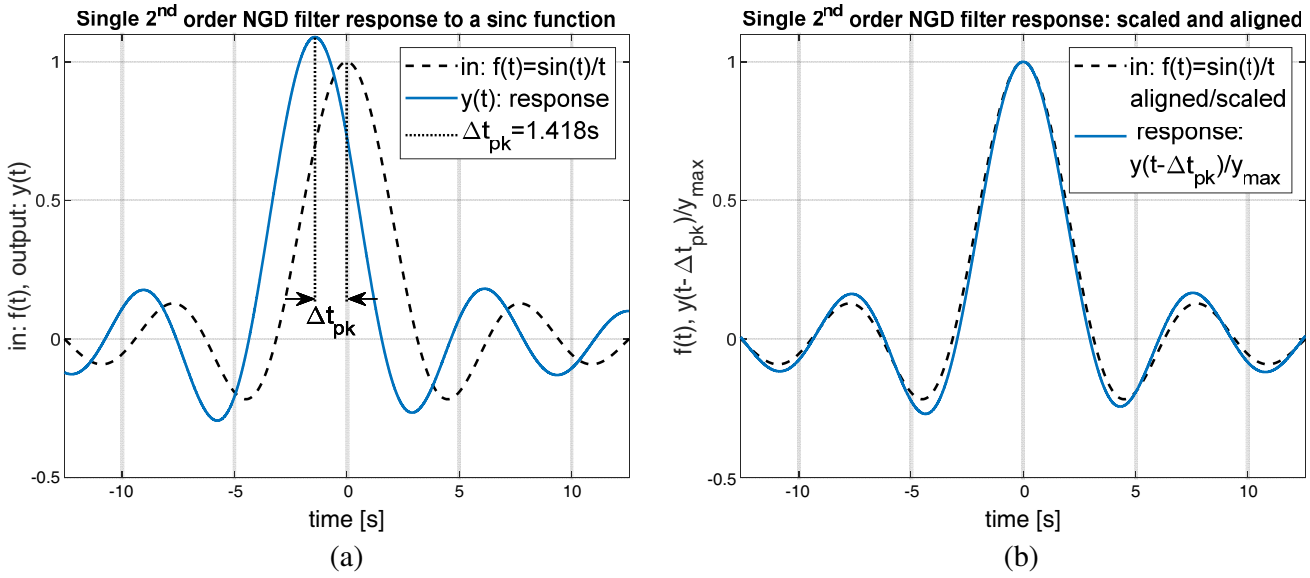

Figure 13. (a) Input sinc function with a corresponding constant frequency spectrum with cut-off at $\omega_c = 1$, and the corresponding output waveform of a single stage 2nd order gain-compensated design. (b) The same comparison but with the output waveform shifted by Δt_{pk} and normalized by $|y(t)|_{\max}$.

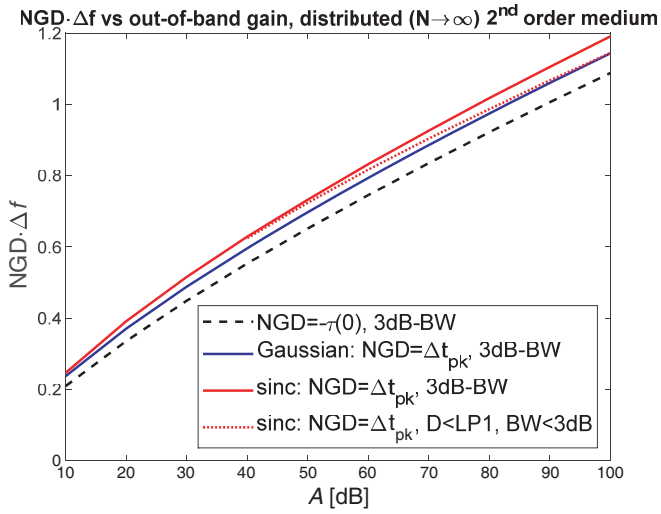

Figure 14. NGD-bandwidth product as a function of out-of-band gain for a distributed 2nd order medium. Frequency domain NGD, as well as time domain NGD for Gaussian and sinc inputs.

from the frequency transfer function, Fig. 14 captures curves obtained when NGD is evaluated from the time-domain response to a Gaussian pulse, as well as the response to a sinc function. For all out-of-band gains considered (up to 100 dB) the distortion of a Gaussian pulse was below that of a single stage 1st-order low-pass design value of $D = 0.0411$. For the sinc function however, the single stage 1st-order low-pass value of $D = 0.1093$ was exceeded for out-of-band gains as low as 40 dB. To keep the distortion level below a desired limit, the effective bandwidth can be reduced below the 3 dB cut-off ω_c, and a wider input sinc function applied that corresponds to the reduced bandwidth. Using this approach, the required bandwidth ranges from $0.995\omega_c$ at $A = 40$ dB, to $0.966\omega_c$ at $A = 100$ dB, in order to keep the distortion factor below the single stage 1st order low-pass value of $D = 0.1093$, for a sinc function input.

Instead of the 3 dB bandwidth (or lower, when distortion metric is above a prescribed level), in some

Table 1. NGD performance metric for N-stage 1st/2nd order baseband topologies.

Number of stages/topology	Out-of-band gain, A [dB]	NGD-BW product, $-\tau(0) \cdot \Delta f_{3\,\mathrm{dB}}$	FOM [1/dB]	$\Delta t_{pk} \cdot \Delta f_{3\,\mathrm{dB}}$ (Gaussian)	$\mathrm{D}_{\text{in-band}}$ (Gaussian)
1× 2nd order	40	0.4052	0.0101	0.4368	0.0217 ($0.53 \times D_{\text{1st-LP-filter}}$)
2× 1st order	40	0.3714	0.0093	0.3544	0.0383 ($0.93 \times D_{\text{1st-LP-filter}}$)
2× 2nd order	40	0.4956	0.0124	0.5336	0.0255 ($0.62 \times D_{\text{1st-LP-filter}}$)
4× 1st order	40	0.4034	0.0101	0.3912	0.0364 ($0.89 \times D_{\text{1st-LP-filter}}$)
distributed 2nd	40	0.5536	0.0138	0.5960	0.0237 ($0.58 \times D_{\text{1st-LP-filter}}$)
distributed 1st	40	0.4182	0.0105	0.4072	0.0357 ($0.87 \times D_{\text{1st-LP-filter}}$)

publications the reported bandwidth of NGD designs spans over the entire frequency range where the group delay response is negative and is typically considerably wider than the 3 dB bandwidth. However, it should be kept in mind that such defined bandwidth is likely to result in a high distortion metric for actual waveforms corresponding to that bandwidth. For example, a single-stage 2nd order NGD circuit presented in this paper exhibits an NGD-bandwidth of 0.4052 when 3 dB bandwidth is considered. Considering the entire bandwidth over which the group delay is negative increases this NGD-bandwidth product over three-fold, to 1.2811. However, for an input Gaussian waveform, the 3 dB bandwidth results in an acceptable distortion metric (53% of the 1st order low pass filter distortion), whereas using the entire bandwidth over which the group delay characteristic is negative would result in an extremely high distortion metric (1,132% of the 1st order low pass filter distortion). This extremely high distortion metric can be explained by plots in Figs. 7(a) and 7(b), which show that the entire bandwidth over which the group delay is negative corresponds to about 20 dB variation in the amplitude characteristic magnitude.

8. CONCLUSION

In this paper, an NGD filter prototype design, based on cascaded identical 2nd order baseband transfer functions, is introduced. The considered baseband transfer function has complex poles and zeros and therefore cannot be reduced to a multiplication of 1st order functions with purely imaginary poles and zeros.

An up-shifted center frequency transfer function is shown to be a 4th order rational function for each 2nd order baseband stage. Factorization of the 4th order upshifted transfer function into two 2nd order functions, reveals two resonant frequencies around the upshifted center frequency. This makes the design possible to implement with a Sallen-Key topology involving RLC parallel resonators tuned to the two resonant frequencies.

The prototype design achieves an NGD-bandwidth product that in the upper asymptotic limit for an infinitely distributed design is a function of out-of-band gain in decibels raised to the power 3/4. This is an improvement of cascaded first-order designs that have an NGD-bandwidth functional dependency of out-of-band gain in decibels to the power of 1/2. The bandwidth is taken as 3 dB amplitude response bandwidth. Out-of-band gain is a trade-off quantity which was shown to be proportional to transient magnitudes [8, 9] for signals with finite turn-on/off instants in time. A figure of merit is introduced that encompasses out-of-band gain and NGD-bandwidth product.

Finally, an in-band distortion metric based on the approach in [12, 13] is presented, for a given time-domain input waveform. If the defined distortion for the proposed 2nd-order prototype filter is to be kept below the corresponding distortion value of a 1st-order low-pass filter, it is shown that the bandwidth has to be reduced below the 3 dB cutoff in some cases for certain types of input waveforms. A sinc input function for example is shown to yield a higher distortion metric compared with a Gaussian pulse, since it has a constant frequency spectrum over the entire bandwidth and therefore equally factors in magnitude and phase distortion across the bandwidth. In addition to the out-of-band gain, the in-band distortion metric constitutes another trade-off quantity (higher NGD-bandwidth designs yield higher in-band distortion) which should be checked for any type of NGD design.

Table 1 shows a performance comparison of selected NGD designs, in terms of their achieved NGD in the frequency domain as well as in the time domain for a given Gaussian input waveform, and the associated FOM and distortion metric. Table 1 depicts values associated with a 3 dB bandwidth, and includes NGD-bandwidth product, corresponding Figure-of-Merit (FOM), time domain Gaussian pulse peak advancement and bandwidth product, corresponding in-band distortion metric $D_{\text{in-band}}$, given for different topologies and a chosen out-of-band gain $A = 40\,\text{dB}$ (or signal attenuation, SA, for passive equivalents). Table 1 includes discrete stage designs as well as infinitely distributed 2nd order (expression 33(a)), and 1st order [8] designs. The distortion metric is lower than the corresponding metric for a 1st order low pass filter, for all considered topologies.

It was demonstrated that selecting a bandwidth which spans over the entire frequency range where the group delay response is negative is likely to result in an unacceptably high distortion metric for actual waveforms corresponding to that bandwidth (over 10 times the distortion metric of a 1st order low pass filter).

ACKNOWLEDGMENT

This work was supported in part by the Natural Sciences and Engineering Research Council of Canada.

REFERENCES

1. Brillouin, L., *Wave Propagation and Group Velocity*, Academic Press, New York, 1960.
2. Mojahedi, M., K. J. Malloy, G. V. Eleftheriades, J. Woodley, and R. Y. Chiao, "Abnormal wave propagation in passive media," *IEEE Journal of Selected Topics in Quantum Electronics*, Vol. 9, No. 1, 30–39, 2003.
3. Stenner, D., D. J. Gauthier, and M. A. Neifeld, "Fast causal information transmission in a medium with a slow group velocity," *Phys. Rev. Lett.*, Vol. 94, No. 5, 053902, 2005.
4. Mojahedi, M., E. Schamiloglu, F. Hegeler, and K. J. Malloy, "Time-domain detection of superluminal group velocity for single microwave pulses," *Phys. Rev. E*, Vol. 62, No. 4, 2000.
5. Wang, Y., Y. Zhang, L. He, F. Liu, H. Li, and H. Chen, "Direct observation of negative phase velocity and positive group velocity in time domain for composite right/left-handed transmission lines," *Journal of Applied Physics*, Vol. 100, 113503, 2006.
6. Ibraheem, A., J. Schoebel, and M. Koch, "Group delay characteristics in coplanar waveguide left-handed media," *Journal of Applied Physics*, Vol. 103, 024903, 2008.
7. Bolda, L., R. Y. Chiao, and J. C. Garrison, "Two theorems for the group velocity in dispersive media," *Phys. Rev. A, Gen. Phys.*, Vol. 48, No. 5, 3890–3894, Nov. 1993.
8. Kandic, M. and G. Bridges, "Asymptotic limits of negative group delay in active resonator-based distributed circuits," *IEEE Trans. Circuits Syst. I*, Vol. 58, No. 8, 1727–1735, Aug. 2011.
9. Kandic, M. and G. Bridges, "Limits of negative group delay phenomenon in linear causal media," *Progress in Electromagnetics Research*, Vol. 134, 227–246, Jan. 2013.
10. Solli, D., R. Y. Chiao, and J. M. Hickmann, "Superluminal effects and negative group delays in electronics, and their applications," *Phys. Rev. E*, Vol. 66, No. 5, 056601, 2002.
11. Dorrah, A. H. and M. Mojahedi, "Nonanalytic pulse discontinuities as carriers of information," *Phys. Rev. A*, Vol. 93, 013823, 2016.

12. Macke, B., B. Ségard, and F. Wielonsky, "Optimal superluminal systems," *Phys. Rev. E*, Vol. 72, 035601(R), 1–4, Sep. 2005.
13. Macke, B. and B. Ségard, "Propagation of light-pulses at a negative group-velocity," *Eur. Phys. J. D*, Vol. 23, 125–141, Feb. 2003.
14. Lucyszyn, S., I. D. Robertson, and A. H. Aghvami, "Negative group delay synthesiser," *Electronics Letters*, Vol. 29, No. 9, 798–800, Apr. 1993.
15. Nakanishi, T., K. Sugiyama, and M. Kitano, "Demonstration of negative group delays in a simple electronic circuit," *Am. J. Phys.*, Vol. 70, No. 11, 1117–1121, Nov. 2002.
16. Kitano, M., T. Nakanishi, and K. Sugiyama, "Negative group delay and superluminal propagation: An electronic circuit approach," *IEEE J. Sel. Topics Quantum Electron.*, Vol. 9, No. 1, 43–51, Feb. 2003.
17. Siddiqui, O. F., M. Mojahedi, and G. V. Eleftheriades, "Periodically loaded transmission line with effective negative refractive index and negative group velocity," *IEEE Trans. Antennas Propag.*, Vol. 51, No. 10, 2619–2625, Oct. 2003.
18. Ravelo, B., A. Perennec, M. Le Roy, and Y. G. Boucher, "Active microwave circuit with negative group delay," *Microwave and Wireless Components Letters*, Vol. 17, No. 12, 861–863, Dec. 2007.
19. Choi, H., Y. Jeong, C. D. Kim, and J. S. Kenney, "Bandwidth enhancement of an analog feedback amplifier by employing a negative group delay circuit," *Progress In Electromagnetics Research*, Vol. 105, 253–272, 2010.
20. Mirzaei, H. and G. V. Eleftheriades, "Realizing non-Foster reactive elements using negative group delay networks," *IEEE Trans. Microw. Theory Techn.*, Vol. 61, No. 12, 4322–4332, Dec. 2013.
21. Chaudhary, G., Y. Jeong, and J. Lim, "Microstrip line negative group delay filters for microwave circuits," *IEEE Trans. Microw. Theory Techn.*, Vol. 62, No. 2, 234–243, Feb. 2014.
22. Wu, C.-T. M. and T. Itoh, "Maximally flat negative group-delay circuit: A microwave transversal filter approach," *IEEE Trans. Microw. Theory Techn.*, Vol. 62, No. 6, 1330–1342, Jun. 2014.
23. Chaudhary, G. and Y. Jeong, "Transmission-type negative group delay networks using coupled line doublet structure," *IET Microw. Antennas Propag.*, Vol. 9, No. 8, 748–754, 2015.
24. Chaudhary, G. and Y. Jeon, "Negative group delay phenomenon analysis using finite unloaded quality factor resonators," *Progress In Electromagnetics Research*, Vol. 156, 55–62, Jan. 2016.
25. Wu, Y., H. Wang, Z. Zhuang, Y. Liu, Q. Xue, and A. Kishk, "A novel arbitrary terminated unequal coupler with bandwidth-enhanced positive and negative group delay characteristics," *IEEE Trans. Microw. Theory Techn.*, Vol. 66, No. 5, 2170–2184, 2018.
26. Wan, F., N. Li, B. Ravelo, and J. Ge, "O=O shape low-loss negative group delay microstrip circuit," *IEEE Trans. Circuits Syst. II, Exp. Briefs*, Vol. 67, No. 10, 1795–1799, Oct. 2020.